Control induced explicit time-scale separation to attain DC voltage stability for a VSC-HVDC terminal

Y. Chen, Gilney Damm, A. Benchaib, Mariana Netto, Françoise Lamnabhi-Lagarrigue

Control induced explicit time-scale separation to attain DC voltage stability for a VSC-HVDC terminal

Yijing Chen[1], Gilney Damm[2], Abdelkrim Benchaib[3], Françoise Lamnabhi-Lagarrigue[1]

***Abstract*— This paper presents a new control scheme to regulate the DC voltage of a VSC terminal. It significantly simplifies the control design process itself and in general also results in an uncomplicated and efficient control architecture. Firstly, an equivalent state space model established in a synchronous dq reference frame is presented. Next we split the overall system into two interconnected subsystems and suppose that different dynamics can be imposed on them under their own sub-controllers. During the design process, we use a reduced model obtained by singular perturbation techniques instead of the original system. The developed control law is actually based on this reduced model and an explicit division of time scales. Simulation results clearly demonstrate that the controller based on the reduced model can regulate the DC voltage with good performances and in the meantime, the real DC voltage can be well approximated by its reduced model.**

I. INTRODUCTION

Today's electricity industry faces a big challenge of developing more flexible and effective technical solutions for power transmission. With the rapid development of power electronics, High Voltage Direct Current (HVDC) systems become more interesting compared to traditional High Voltage Alternative Current (HVAC) systems. The applications of HVDC systems are specially suited to [1]:

- economically transmit large amounts of electrical energy over long distances via overhead lines or cables,
- transfer the energy through underwater power cables with lower electrical losses and smaller costs,
- connect asynchronous AC grids and allow power transmission between them,
- feed weak AC networks, for example, providing power supplier to isolated islands.

HVDC systems are usually divided into two main categories. Early HVDC systems were built up with line commutated converters (LCC) where each valve has a number of thyristors connected in series. The main drawback of LCC is that the converter has only one degree of freedom, i.e. the firing angle. Thus the DC current direction usually can't change. In addition the converter always consumes reactive power irrespective of the power direction and some considerable harmonic distortion may be produced and then injected to the AC side of the converter. In order to overcome these shortcomings, an attractive alternative for HVDC systems is developed called as voltage-sourced converters (VSC) owing a second degree of freedom. The additional controllability brings many advantages, especially the ability to control the reactive power independently of the active power, to improve the harmonic performance and to realize the bidirectional power transmission.

This paper mainly concerns the control design for a VSC terminal with the application of Pulse Width Modulation (PWM) technology [2]. As mentioned before, a VSC terminal possesses two degrees of freedom which means that there are maximum two possible controllable outputs. Hence, different control strategies exist [3], for instance, active-reactive power terminal control, DC voltage-reactive power terminal control, active power-AC voltage terminal control etc. There have already been several studies on the control design for VSC HVDC systems [4]-[10]. A discrete-time sliding mode control of a VSC based STATCOM is presented in [9]. Alternatively in [6], [8], control systems for multi-terminal VSC-HVDC transmission are developed. In [5] the author gives a nonlinear state feedback controller to control a Back to Back HVDC system and [10] proposes a control scheme in unbalanced network condition.

In this work we address the problem of regulating the DC voltage and the reactive power. Firstly, an equivalent averaged state space model is introduced established in a synchronous dq reference frame [5]. The system is similar to an underactuated mechanical system [11] with fewer control inputs than state variables. In previous studies we have discussed the nonlinear control of a VSC terminal by means of feedback linearization theory and presented some results where we have derived and analyzed the zero dynamics which play a pivotal role to determine the stability of the system [12], [13], [14]. In the present paper, we develop a new control structure based on a reduced model. Suppose that the system can be divided into two interconnected subsystem, i.e. the current subsystem and the DC voltage subsystem where the current subsystem can have faster dynamics in contrast with the DC voltage subsystem. Then a reduced model is deduced for the DC voltage subsystem, only bored on the slower time scale. Instead of designing the control law for the original DC voltage subsystem, we develop the controller based on the reduced model. This greatly simplifies the control design process. Simulation results show that the real DC voltage subsystem can be well approximated by its reduced model and the considered variables are also regulated with good performances under

This work is supported by the French national project WINPOWER (ANR-10-SEGI-016).

[1]Y. Chen and F. Lamnabhi-Lagarrigue are with Laboratoire des Signaux et Systèmes (LSS), Supélec, 3 rue Joliot-Curie, 91192 Gif-sur-Yvette, France (tel: +33 1 69 85 17 77, e-mail: yijing.chen@lss.supelec.fr, francoise.lamnabhi-lagarrigue@lss.supelec.fr).

[2]G. Damm is with Laboratoire IBISC, Université d'Evry-Val d'Essonne, 40 rue du Pelvoux, 91020 Evry, France (e-mail: gilney.damm@ibisc.fr).

[3]A. Benchaib is with ALSTOM GRID/CNAM, France (e-mail: abdelkrim.benchaib@alstom.com).

the proposed controller.

II. VSC TERMINAL MODELING

A VSC terminal is shown in Fig.1 connected to an AC network via the phase reactor which has large inductance L_l with small resistance R_l. It dominates the dynamic behavior on the AC side of the converter. The DC voltage u_c is provided by the DC capacitor C whose size determines the dynamic behavior on the DC side. It is assumed that the AC network is strong enough such that its voltages $v_{l,dq}$ at the point of common coupling (PCC) remain constant regardless of the magnitude and direction of active and reactive power flow. $v_{c,dq}$ are the converter voltages, $i_{l,dq}$ are the currents through the phase reactor, i_d is the converter's DC side current and i_c is the DC bus current representing the active power demand/supply from the HVDC grid.

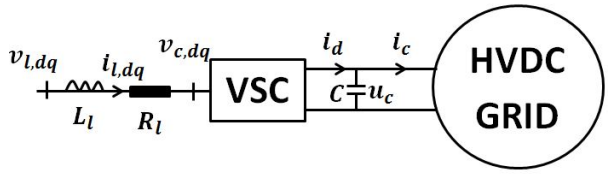

Fig. 1. A VSC terminal.

According to Kirchhoff voltage law, the voltage drop through the reactor phase satisfies:

$$v_{l,abc} - v_{c,abc} = R_l i_{l,abc} + L_l \frac{di_{l,abc}}{dt} \tag{1}$$

By considering the balanced three phase system rotating at a frequency ω, system (1) is transformed to a rotating dq reference frame as:

$$\frac{di_{ld}}{dt} = -\frac{R_l}{L_l} i_{ld} + \omega i_{lq} + \frac{v_{ld}}{L_l} - \frac{v_{cd}}{L_l} \tag{2}$$

$$\frac{di_{lq}}{dt} = -\frac{R_l}{L_l} i_{lq} - \omega i_{ld} + \frac{v_{lq}}{L_l} - \frac{v_{cq}}{L_l} \tag{3}$$

With Pulse Width Modulation (PWM) technology, the magnitude of the converter voltage can be regulated by the modulation index M_{dq} as:

$$v_{c,dq} = \frac{1}{2} M_{dq} u_c \tag{4}$$

where M_{dq} are limited to $\sqrt{M_d^2 + M_q^2} \leq 1$.

The DC circuit of a VSC terminal owns a large capacitor C as seen in Fig.1. Its basic equation is

$$C\frac{du_c}{dt} = i_d - i_c \tag{5}$$

Because of the power balance on both sides of the converter, we have:

$$u_c i_d = \frac{3}{2}(v_{cd} i_{ld} + v_{cq} i_{lq}) \tag{6}$$

By substituting (4) and (6) into (2), (3) and (5), the global continuous-time equivalent mathematical model of the VSC terminal is obtained by:

$$\frac{di_{ld}}{dt} = -\frac{R_l}{L_l} i_{ld} + \omega i_{lq} + \frac{v_{ld}}{L_l} - \frac{u_c}{2L_l} M_d \tag{7}$$

$$\frac{di_{lq}}{dt} = -\frac{R_l}{L_l} i_{lq} - \omega i_{ld} + \frac{v_{lq}}{L_l} - \frac{u_c}{2L_l} M_q \tag{8}$$

$$\frac{du_c}{dt} = -\frac{1}{C} i_c + \frac{3}{4C}(M_d i_{ld} + M_q i_{lq}) \tag{9}$$

with the active and reactive powers P_l and Q_l:

$$P_l = \frac{3}{2}(v_{ld} i_{ld} + v_{lq} i_{lq}); \quad Q_l = \frac{3}{2}(v_{lq} i_{ld} - v_{ld} i_{lq}) \tag{10}$$

For the sake of simplicity, the synchronous dq reference frame is chosen such that the d-axis is fixed to the AC area voltage, i.e. $v_{ld} = V_{l,rms}$ and $v_{lq} = 0$ and hence the decoupled control on P_l and Q_l can be realized:

$$P_l = \frac{3}{2} v_{ld} i_{ld}; \quad Q_l = -\frac{3}{2} v_{ld} i_{lq} \tag{11}$$

III. CONTROL STRUCTURE

A. Control objective

The control objective is to make the DC voltage u_c and the reactive power Q_l track their desired values u_c^* and Q_l^* which are provided by a higher control level. As seen in (11), Q_l is directly regulated by i_{lq}. In order to simplify the problem, we introduce a reference value i_{lq}^* for i_{lq}, where i_{lq}^* satisfies:

$$i_{lq}^* = -\frac{2}{3}\frac{Q_l^*}{v_{ld}} \tag{12}$$

B. Control design

In this paper, the control design is inspired by the nonlinear control structure proposed in [2]. It is mainly based on the following consideration:

- The global model (7)-(9) can be seen as two interconnected subsystems, i.e. the dq current subsystem $S1$ and the DC voltage subsystem $S2$. It is known that, if $S1$ and $S2$ are stable, the overall system may not be. Therefore, it is necessary to develop a control strategy such that we can separately shape the behaviors of $S1$ and $S2$, while ensuring the stability of the overall system.

Defining $x_{1,2} \triangleq (i_{ld},\ i_{lq})^T$, $z \triangleq u_c$, $u_{1,2} \triangleq (M_d,\ M_q)^T$, the system (7)-(9) can be written as:

$$\dot{x} = f_x(x,\ z) + g_x(x,\ z)u \tag{13}$$

$$\dot{z} = f_z(x,\ z) + g_z(x,\ z)u \tag{14}$$

with the obvious expressions for $f_x(x,\ z)$, $g_x(x,\ z)$, $f_z(x,\ z)$ and $g_z(x,\ z)$.

The system is a third order system with two control inputs and hence, only two variables can be controlled directly and the remaining may be brought to an equilibrium state via those controllable variables. As seen in (13) and (14), x and u have the same dimension and furthermore, x can be considered collocated with the control input u. It is natural to consider that we first develop a control law for u to force x into converging to a reference trajectory x^* yet to be

designed. In our case, we have i_{lq}^* and u_c^* but there is no ready-made i_{ld}^* for i_{ld}. Consequently, the determination of i_{ld}^* is a crucial step. In this paper, we show that i_{ld}^* can be developed via a simpler reduced model in two steps:

1) current subsystem design: By considering the current subsystem (13), suppose that there exits a state feedback control law for $u = h_1(x,\ z)$ such that x at least locally exponentially converges to x^* as follows:

$$\begin{aligned}\dot{x} &= f_x(x,\ z) + g_x(x,\ z)h_1(x,\ z)\\ &= A\tilde{x} + r(x)\end{aligned} \tag{15}$$

where $\tilde{x} = x - x^*$ and A is a designed linear and Hurwitz matrix. It is known that, for any nonlinear system $\dot{x} = f(x)$ where f is a continuous differential map, it can be divided into a linear part and a nonlinear part. The nonlinear part converges to zero when the state variables converge to their equilibrium values. In our case, $r(x)$ satisfies

$$\frac{||r(x)||}{||\tilde{x}||} \to 0 \ as \ ||\tilde{x}|| \to 0 \tag{16}$$

The nonlinear part is usually used to improve the performances of the system, for instance making the overall system more robust if there are some errors of the measurements or uncertainties of the parameters.

For a nonlinear system, its behaviors are dominated by its linear part in a small neighborhood of the equilibrium point. Therefore, we can impose fast dynamics on the current subsystem by designing A and then $h_1(x,\ z)$ can be obtained by solving (15):

$$h_1(x,\ z) = g_x^{-1}[A\tilde{x} + r(x) - f_x] \tag{17}$$

under the condition that g_x is nonsingular.

It is noticed that the control law $h_1(x,\ z)$ would be explicitly a function of $(x,\ z,\ x^*)$ without the term $\frac{dx^*}{dt}$ if it is supposed that x^* varies much slower compared to x. Hence, when designing x^*, we must impose slow dynamics for it compared to the remaining system. In this paper, i_{lq}^* is a known constant with $\frac{di_{lq}^*}{dt} = 0$. The coming task is to design a slow varying i_{ld}^* such that $\frac{di_{ld}^*}{dt}$ has negligible effects on the current subsystem.

2) DC voltage subsystem design: Let us suppose the current subsystem, x will quickly enter the manifold $x = x^*$ steered by (17). Then the control input becomes

$$u_{re} = h_1(x^*,\ z) = -g_x^{-1}(x^*,\ z)f_x(x^*,\ z) \tag{18}$$

Considering that during the first step x converges to x^* very fast and then substituting $x = x^*$ and $u = u_{re}$ into (14), we obtain "a reduced model ":

$$\dot{z} = f_z(x^*,\ z) - g_z(x^*,\ z)g_x^{-1}(x^*,\ z)f_x(x^*,\ z) \tag{19}$$

Denote the solution of (19) as z_{re}, our goal is to develop a control law such that z_{re} converges to z^*. Regarding the reduced model (19), its state variable is expected to be regulated by the control trajectory x^*, i.e. regulate u_c by i_{ld}^* . As done in III-B.1, suppose that there exists a state feedback control law $x^* = h_2(z)$ such that z in (19) at least is locally asymptotically stabilized at z^* and then we have:

$$\dot{z} = f_z(h_2(z), z) - g_z(h_2(z), z)g_x^{-1}(h_2(z), z)f_x(h_2(z), z) \tag{20}$$

$$= A_{re}(z - z^*) + r_{re}(z) \tag{21}$$

where A_{re} is a designed linear and Hurwitz matrix, $r_{re}(z)$ represents the nonlinear part and satisfies:

$$\frac{||r_{re}(z)||}{||z - z^*||} \to 0 \ as \ ||z - z^*|| \to 0 \tag{22}$$

and hence $h_2(z)$ can be deduced by combining (20) and (21). Now we introduce an additional integrator in x^* as:

$$\frac{dx^*}{dt} = v_x \tag{23}$$

which yields a higher order reduced model as:

$$\frac{dz}{dt} = f_z(x^*,\ z) - g_z(x^*,\ z)g_x^{-1}(x^*,\ z_{re})f_x(x^*,\ z) \tag{24}$$

$$\frac{dx^*}{dt} = v_x \tag{25}$$

By combing (20), (21), (24) and (25), the reference x^* sent to the current subsystem is designed as:

$$x^* = h_2(z) \tag{26}$$

It can be summarized that the overall control structure for the original system (13)-(14) consists of (17) and (26). The best we can expect is that the solution of the original system z approaches the solution of the reduced model. The crucial point is to design A and A_{re} such that they dominate the convergence speeds of x and z in their small neighborhoods, respectively. It can be proved by a singular perturbation approach that if A is designed making the convergence speed of x much faster, the errors between z and z_{re} becomes smaller. For length limitations, a detailed demonstration will not be presented here and will be described in a longer paper.

C. Application to the VSC terminal

The proposed example is to chose A as a diagonal matrix and $r(x) = 0$ which means that i_{ld} and i_{lq} can be controlled independently and then M_{dq} are deduced as:

$$\begin{pmatrix} M_d \\ M_q \end{pmatrix} = -\begin{pmatrix} \frac{2L_l}{u_c} & 0 \\ 0 & \frac{2L_l}{u_c} \end{pmatrix} \cdot \left(\begin{pmatrix} -k_d & 0 \\ 0 & -k_q \end{pmatrix} \begin{pmatrix} i_{ld} - i_{ld}^* \\ i_{lq} - i_{lq}^* \end{pmatrix} - \begin{pmatrix} -\frac{R_l}{L_l} i_{ld} + \omega i_{lq} + \frac{v_{ld}}{L_l} \\ -\frac{R_l}{L_l} i_{lq} - \omega i_{ld} + \frac{v_{lq}}{L_l} \end{pmatrix} \right) \tag{27}$$

with positive k_d and k_q used to regulate the convergence speeds of i_{ld} and i_{lq}. Substitute the resulting expression (27) into (9) and then obtain the reduced model as:

$$\dot{u}_c = -\frac{i_c}{C} + \frac{3}{2C}\frac{(-R_l i_{ld}^{*^2} + v_{ld} i_{ld}^*) + (-R_l i_{lq}^{*^2} + v_{lq} i_{lq}^*)}{u_c} \tag{28}$$

where the term $i_{ld}^{*^2}$ explicitly appears. As mentioned above, an additional integrator is introduced as:

$$\frac{di_{ld}^*}{dt} = u_d \tag{29}$$

In order to make u_c in (28) converge to u_c^*, several control techniques can be used. Here we apply Input/Output feedback linearization theory, u_c is considered as the output and the relative degree of it is two. The following Lie derivative can be deduced:

$$\dot{u}_c = L_{f_0}^1(u_c) \tag{30}$$

$$\ddot{u}_c = L_{f_0}^2(u_c) + L_{g_0} L_{f_0}^1(u_c) u_d \tag{31}$$

where

$$L_{f_0}^1(u_c) = -\frac{i_c}{C} + \frac{3}{2C} \times \frac{(-R_l i_{ld}^{*^2} + v_{ld} i_{ld}^*) + (-R_l i_{lq}^{*^2} + v_{lq} i_{lq}^*)}{u_c} \tag{32}$$

$$L_{f_0}^2(u_c) = -\frac{3L_{f_0}^1(u_c)}{2C}\frac{(-R_l i_{ld}^{*^2} + v_{ld} i_{ld}^* + -R_l i_{lq}^{*^2} + v_{lq} i_{lq}^*)}{u_c^2} \tag{33}$$

$$L_{g_0} L_{f_0}^1(u_c) = \frac{3}{2C}\frac{1}{u_c}(-2R_l i_{ld}^* + v_{ld}) \tag{34}$$

By introducing an auxiliary input θ_d, u_d is designed as

$$u_d = \frac{1}{L_{g_0} L_{f_0}^1(u_c)}(-L_{f_0}^2(u_c) + \theta_d) \tag{35}$$

where θ_d is chosen using linear techniques as:

$$\theta_d = -c_1(u_c - u_c^*) - c_2 \dot{u}_c \tag{36}$$

with positive c_1 and c_2. By substituting (35) and (36) in (28) and (29), the closed loop system for the reduced model can be written as:

$$\frac{d}{dt}\begin{pmatrix} u_c \\ \dot{u}_c \end{pmatrix} = \begin{pmatrix} 0 & 1 \\ -c1 & -c2 \end{pmatrix}\begin{pmatrix} u_c - u_c^* \\ \dot{u}_c \end{pmatrix} \tag{37}$$

where c_1 and c_2 determine the convergence speed of the reduced model. Finally i_{ld}^* is developed satisfying:

$$\frac{di_{ld}^*}{dt} = -\frac{L_{f_0}^2(u_c) + c_1(u_c - u_c^*) + c_2 \dot{u}_c}{L_{g_0} L_{f_0}^1(u_c)} \tag{38}$$

As seen in (37), the resulted closed loop system is a linear second order system and by allocation c_1 and c_2, we can impose slow dynamics on the reduced model.

In the proposed scenario, feedback linearization approach is chosen since linear system properties can be applied to help us control the behaviour of the system.

Terminal	R_l	L_l	v_{ld}	C	f
	0.05 Ω	40e-3 H	140 kV	20e-3 F	50 Hz

TABLE I

PARAMETER VALUES OF THE VSC TERMINAL.

IV. SIMULATION RESULTS

The proposed DC voltage control structure has been implemented for the VSC terminal shown in Fig.1 in Matlab/Simulink environment. System parameters are given in Table I. In order to obtain an unitary power factor, i_{lq}^* is set to zero during the entire simulation process.

In this paper, three simulated scenarios are considered where the system initially operates in a steady state with a rated DC transmission voltage $u_c^* = 300$ KV, $i_c = 700$ A, $i_{ld} = 1000$ A and $i_{lq} = 0$.

Scenario 1: the choice of control gains

As mentioned in Part III, the control structure is based on the current subsystem having faster dynamics than the DC voltage subsystem. In this part, we will present the influences of the control gains on the behaviors of the system. At $t = 5$s, it is desired to have a step of 40% increase in the DC voltage reference value, i.e. $u_c^* = 420$ KV. Two sets of control gains are tested as follows:

Control gains in the current subsystem larger than those in the DC voltage subsystem: Figs.2 show simulation results with two sets of control gains: $k_{d1} = k_{q1} = 50$ (dashed) and $k_{d2} = k_{q2} = 150$ (solid). In addition, c_1 and c_2 are set to 15^2 and 15, respectively. Fig.2(a) shows u_c responses and Fig.2(b) shows the DC voltage errors between u_c from the real model and $u_{c,re}$ from the reduced model. The blue and red lines stand for a stable range of $\pm 2\%$ of the step change in DC voltage reference value. It is observed that the time required for both responses of u_c to stay within this range are less than 1.5s. Moreover, the performances of u_{c2} with larger $k_{dq,2}$ are better than those of u_{c1} with smaller $k_{dq,1}$. As seen in Fig.2(a), u_{c2} reaches the stable range around $t = 6$s while u_{c1} around $t = 6.1$s. Furthermore, the response of u_{c2} are closer to $u_{c,re}$ in comparison with u_{c1} shown in Fig.2(b). This illustrates that the controller works better if the dynamics of these two subsystems are imposed far apart. In the next two simulated scenarios, the control gains are chosen as $k_d = k_q = 150$ and $c_1 = 15^2,\ c_2 = 15$.

Scenario 2: Variations in i_c

As previously described, i_c is the measurable DC bus current representing the DC power demand/supply from the HVDC grid. Suppose that the power injections from other terminals may be time-varying or be subjected to certain sudden step changes, for instance, adding or removing loads. These events will drive the HVDC grid in power imbalance and lead to the variations in i_c. In order to balance the active power, it is proposed that the terminal responsible for regulating the DC voltage transmission level works as a slack bus. In this scenario, we will test if the proposed controller

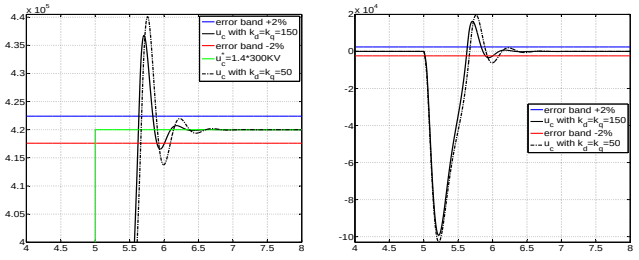

(a) u_c response (b) Errors between u_c and $u_{c,re}$

Fig. 2. $k_d = k_q = 50$ (dashed) and $k_d = k_q = 150$ (solid).

can make the terminal well operate in the role of slack bus. The sequence of events of i_c applied to the VSC terminal is illustrated in Fig.3(a) and the responses of related variables are depicted in Fig.3(b)-3(f).

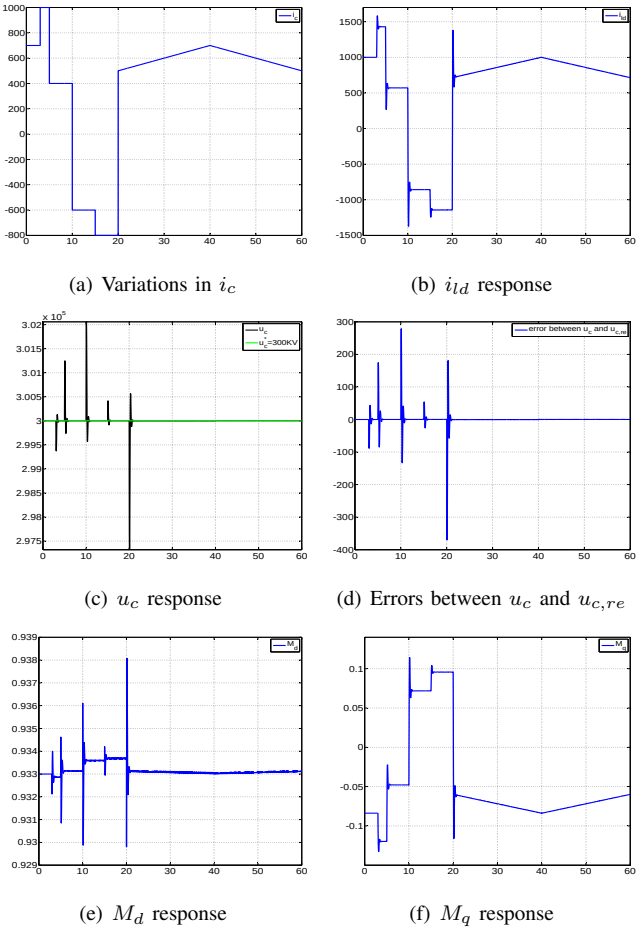

(a) Variations in i_c (b) i_{ld} response

(c) u_c response (d) Errors between u_c and $u_{c,re}$

(e) M_d response (f) M_q response

Fig. 3. Responses of related variables with varying i_c.

The system initially operates in rectification mode with a positive $i_c = 700$ A and $u_c^* = 300$ KV. At $t = 3$s, i_c is augmented to 1000 A due to the increase in power demand from the HVDC grid. As shown in Fig.3(b), i_{ld} gives a corresponding response and reaches a new steady state around 1429.5 A. At $t = 5$s, i_c suddenly drops to 400 A since certain loads may be removed from other terminals. Now i_{ld} is stable around 571.3 A. During $t \in (0, 10)$s, despite having small overshoots u_c can be still quickly stabilized at its rated level $u_c^* = 300$ KV shown in Fig.3(c). These two actions demonstrate that the terminal has good performances in rectification mode.

At $t = 10$s, let the terminal operate from rectification mode to inversion mode by reversing the direction of i_c and setting it to -600 A. i_{ld} is reversed as well and arrives at a new equilibrium value -857.5 A. During this process, u_c is finally well regulated at 300 KV after a transient change. From this event, we see that the terminal can realize the bidirectional power transmission. At $t = 15$s, i_c abruptly decreases to -800 A and i_{ld} droops to a corresponding steady point -1143.5 A as well. It is shown that the terminal works well in inversion mode.

Now, suppose that the other terminals are connected with some renewable energy sources, for instance, wind farms from $t = 20$s. It is known that the production of wind farms are strongly related to the speed of the wind and hence, i_c may be time-varying. In this paper i_c is simply simulated as a ramp with slope $k = 20$ during the interval $t \in (20, 40)$s because of the increase in wind speed and then with another slope $k = -20$ during $t \in (40, 60)$s caused by the decrease in wind speed. In Fig.3(b), i_{ld} first gradually increases from 732 A until 1000 A at $t = 40$s and then decreases back to 732 A at $t = 60$s. During this event, u_c just slightly changes and is always regulated at 300 KV with excellent performances. It is illustrated that the terminal can well operate even though i_c varies.

As shown in Fig.3(e)-3(f), the control inputs M_{dq} always stay in their feasible region satisfying $\sqrt{M_d^2 + M_q^2} \leq 1$. In addition, the errors between u_c and $u_{c,re}$ depicted in Fig.3(d) still converge to zero fast enough with small overshoots regardless of any variation in i_c. It means that u_c can be well approximated by $u_{c,re}$.

Scenario 3: Step changes in DC voltage transmission level

One important characteristic of developing HVDC systems via VSCs is the ability of changing the DC working voltage. In this part, we will test the performances when gradually increasing or decreasing the DC voltage transmission level.

Fig.4 shows the response of u_c (black) with varying u_c^* (green) who has a $1\% \times 300$ KV step change every two seconds and its positive/negative error bands (blue and red). At $t = 2$s, a new reference value $u_c^* = 303$ KV is given and then u_c starts to increase as seen in Fig.4(a) and before $t = 2.57$, u_c remains in the stable region $u_c \in (-2\% \times 1\% \times 300 + 303, 2\% \times 1\% \times 300 + 303)$ KV, i.e. the region between these two error bands. In the meantime, i_{ld} attains a new steady state around 1010 A as shown in Fig.5(a). At $t = 4$s and $t = 6$s, the DC voltage reference value continues to increase with the same step change, i.e. $1\% \times 300$ KV, respectively. It is seen that u_c gives a fast response to follow these new reference values and i_{ld} has a related response in accordance with the change of u_c. Conversely, at $t = 8$s u_c^* is required to decrease 1%. Under the proposed controller,

u_c is well regulated around the new reference value and i_{ld} droops to a new steady point as well.

It can be seen that the errors between u_c and $u_{c,re}$ converge to zero with slight variations as presented in Fig.5(b). From Figs.5(c)-5(d), M_{dq} always remain in their feasible region.

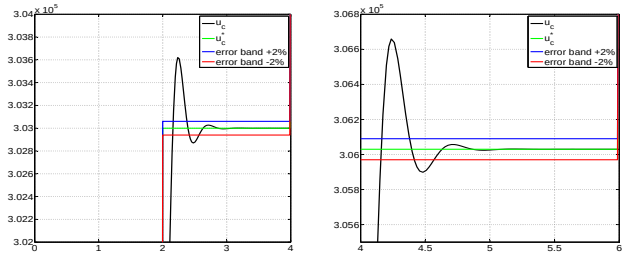

(a) t = 0s-4s

(b) t = 4s-6s

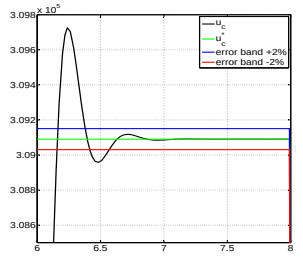

(c) t = 6s-8s

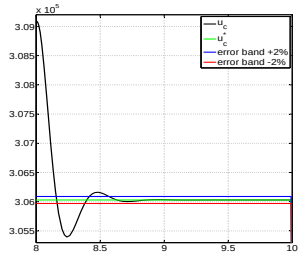

(d) t = 8s-10s

Fig. 4. u_c response with varying u_c^*.

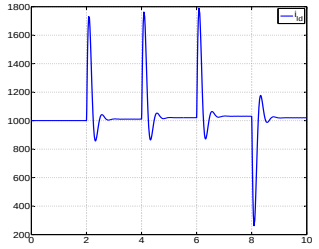

(a) i_{ld} response

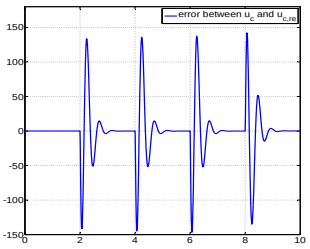

(b) Error between u_c and $u_{c,re}$

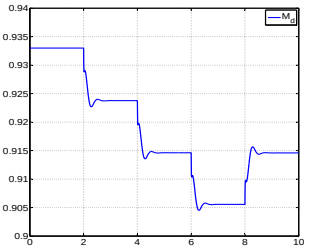

(c) M_d response

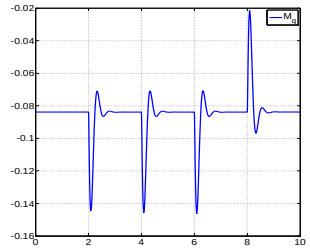

(d) M_q response

Fig. 5. Responses of related variables with varying u_c^*.

Additionally, i_{lq} not presented in this paper indeed is always controlled at zero during these three scenarios. From the above simulation results, we conclude that the DC voltage can be well-regulated and can cope with the variations either in i_c or in u_c^*.

V. Conclusions

An efficient DC voltage controller for the VSC terminal is developed in this paper. In brief, the control structure consists of two parts. The first part is used to impose fast dynamics on the current subsystem and the second part is designed to make the DC voltage have slow dynamics. When the dq currents quickly enter their desired manifolds, the DC voltage is then brought into a reduced manifold. Instead of developing a control law for the real DC voltage subsystem, we design a control strategy based on the reduced model and then apply it to the real DC voltage subsystem since it is usually easier to develop a controller for the reduced model. Simulation results clearly show that the real DC voltage subsystem can be well approximated by its reduced model since the time scales are designed well apart. The proposed controller based on the reduced model can regulate u_c with good performances regardless of the variations in i_c and u_c^*.

In this paper, part of the control law for the reduced model is based on feedback linearization since linear system theory can be easily applied to determine the behaviors. In future work, it is proposed to apply other approaches to design these subcontrollers.

References

[1] "Alstom Grid: HVDC transmission systems." http://www.alstom.com/grid/products-and-services/engineered-energy-solutions/hvdc-transmission-systems/.

[2] A. Lindberg and T. Larsson, "PWM and control of three level voltage source back-to-back station," 1996.

[3] C. Du, "The control of VSC-HVDC and its use for large industrial power systems," 2003.

[4] Y. Chen, J. Dai, G. Damm, F. Lamnabhi-Lagarrigue, *et al.*, "Nonlinear control design for a multi-terminal VSC-HVDC system," in *Proceedings of the European Control Conference*, 2013.

[5] J. L. Thomas, S. Poullain, and A. Benchaib, "Analysis of a robust DC-bus voltage control system for a VSC transmission scheme," in *Seventh International Conference on AC and DC Transmission*, (London), November 2001.

[6] J. Liang, O. Gomis-Bellmunt, J. Ekanayake, N. Jenkins, and W. An, "A multi-terminal hvdc transmission system for offshore wind farms with induction generators," *International Journal of Electrical Power & Energy Systems*, vol. 43, no. 1, pp. 54–62, 2012.

[7] O. Gomis-Bellmunt, A. Junyent-Ferré, A. Sumper, and J. Bergas-Jané, "Control of a wind farm based on synchronous generators with a central hvdc-vsc converter," *Power Systems, IEEE Transactions on*, vol. 26, no. 3, pp. 1632–1640, 2011.

[8] H. Chen, C. Wang, F. Zhang, and W. Pan, "Control strategy research of VSC based multiterminal HVDC system," in *IEEE PES Power Systems Conference and Exposition. PSCE '06*, pp. 1986–1990, November 2006.

[9] J. Eloy-Garcia, S. Poullain, and A. Benchaib, "Discrete-time sliding-mode control of a STATCOM including voltage and current limitations for wind farm applications," in *Power Electronics and Motion Control Conference, 2006. EPE-PEMC 2006. 12th International*, pp. 1448–1453, IEEE, 2006.

[10] S. Poullain, E. Courbon, and J. Thomas, "VSC-HVDC robust control scheme in unbalanced network conditions," in *10th European Conference on Power Electronics and Applications, Toulouse*, 2003.

[11] M. W. Spong, "Underactuated mechanical systems," in *Control Problems in Robotics and Automation*, pp. 135–150, Springer, 1998.

[12] A. Isidori, *Nonlinear Control Systems, Third Edition*. Springer, 1995.

[13] H. Khalil, *Nonlinear Systems*. New Jersey: Prentice Hall, 3rd ed., 1996.

[14] R. Marino and P. Tomei, *Nonlinear control design: geometric, adaptive and robust*. Prentice Hall International (UK) Ltd., 1996.